BELLE2-NOTE-PH-2024-XXX
Version 0.0
April 12, 2025

Study of branching fractions and CP asymmetry of $B^+ \to \eta\rho^+$ decays at Belle and Belle II

M.-C. Chang* and K.-Y. Wu

Fu Jen Catholic University

Abstract

We obtain the number of expected events of $B^+ \to \eta\rho^+$ at the signal MC events for Belle II. The number of expected events of decay mode $B^+ \to \rho^+\eta_{\gamma\gamma}$ is xxxx and that of decay mode $B^+ \to \rho^+\eta_{\pi\pi\pi^0}$ is xxxx. The total number of expected events is xxxx. The uncertainties are statistical. The ultimate goal is to measure the branching fractions and CP asymmetry in $B^+ \to \eta\rho^+$, B^+B^- pairs collected with Belle and Belle II. The study is based on a data sample that contains 711 fb^{-1}, 771×10^6 $B\bar{B}$ pairs, collected with the Belle detector at the KEKB asymmetric energy e^+e^- (3.5 GeV and 8 GeV) collider. Also, we use the dataset that contains 362 fb^{-1}, 387×10^6 $B\bar{B}$ pairs, collected by the Belle II detector in 2019-2022 at the Super KEKB at the $\Upsilon(4S)$ center of mass energy e^+e^- (4 GeV and 7 GeV) collider.

*Electronic address: jeri.mcchang@gmail.com

Contents

1. INTRUDUCTION

Charmless two-body decays of B mesons are a powerful probe for testing the standard model (SM) and searching for new physics phenomena. Decays to final states containing η or η' mesons exhibit a distinctive pattern of interference among the dominant amplitudes and are also sensitive to a potentially large flavor-singlet contribution[1]. B meson decays to the final states $\eta\rho^+(770)$ and have been investigated theoretically within the SM by means of perturbative QCD (pQCD)[2], QCD Factorization (QCDF)[3], Soft Collinear Effective Theory (SCET)[4], and SU(3) flavor symmetry[5].

In previous measurements, Belle reported the upper limits for the branching fraction to be $\mathcal{B}(B^+ \to \eta\rho^+) = 4.1 \pm^{1.4}_{1.3} \pm 0.4 \times 10^{-6}$ with 449×10^6 $B\overline{B}$ pairs [6], while BaBar reported the measurement of the branching fraction $\mathcal{B}(B^+ \to \eta\rho^+) = (9.9 \pm 1.2 \pm 0.8) \times 10^{-6}$ with 459×10^6 $B\overline{B}$ pairs[7]. The previous measurements are performed by Belle and BaBar. The results from BaBar and Belle show poor agreement. Updating the branching fraction of these channels at Belle/Belle II is crucial for comparing and discriminating between various model portfolios.

In this note, we report study of the branching fractions of B mesons decaying to the final states $\eta'\rho^+(770)$ and $\eta\rho^+(770)$. Where applicable, we also measure the charge asymmetry $A_{ch} \equiv (\Gamma^- - \Gamma^+)/(\Gamma^- + \Gamma^+)$, where the superscript to the decay width Γ refers to the charge of the B^+ meson decays.

2. DATA SAMPLES

The study is based on a data sample that contains 711 fb^{-1}, 771×10^6 $B\bar{B}$ pairs, collected with the Belle detector at the KEKB asymmetric energy e^+e^- (3.5 GeV and 8 GeV) collider. Also, we use the dataset that contains 362 fb^{-1}, 387×10^6 $B\bar{B}$ pairs, collected by the Belle II detector in 2019-2022 at the Super KEKB at the $\Upsilon(4S)$ center of mass energy e^+e^- (4 GeV and 7 GeV) collider.

The data and Monte Carlo (MC) samples of Belle and Belle II shown in TABLE I and TABLE II have been used for the study.

	Sample size
Signal MC	private generated MC
$e^+e^- \to q\bar{q}$	1 streams of $\mathcal{L}_{int}^{\text{Belle}}$
Generic B MC	1 streams of $\mathcal{L}_{int}^{\text{Belle}}$
Rare B MC	$50 \times \mathcal{L}_{int}^{\text{Belle}}$
Data	771×10^6 $B\bar{B}$

TABLE I: MC samples and data - Belle

	Sample available
Signal MC	4M signal MC15rd
Generic MC	1.4 ab^{-1}
($e^+e^- \to q\bar{q}$, $\Upsilon(4S) \to B\overline{B}$)	
Data	387×10^6 $B\bar{B}$ [$\mathcal{L} = 362 fb^{-1}$]

TABLE II: MC samples and data- Belle II

3. EVENT SELECTION-BELLE II

3.1. Reconstruction

The signal MC events for Belle II use the decay tables shown below. We generated 100k events, of which 50k are for $B^+ \to \eta(\to \pi^+\pi^-\pi^0)\rho^+(\to \pi^+\pi^0)$ and the other 50k are for $B^+ \to \eta(\to \gamma\gamma)\rho^+(\to \pi^+\pi^0)$. The sub-branching fractions which come from PDGLive[8] are listed in the TABLE ??. These values will be used later when calculating the expected number of events.

```

Alias      etasig     eta
ChargeConj etasig     etasig

Alias       rho+sig    rho+
Alias       rho-sig    rho-
ChargeConj  rho+sig    rho-sig

Alias      pi0sig     pi0
ChargeConj pi0sig     pi0sig

#

Decay Upsilon(4S)
0.5  B+sig   B-   VSS;
0.5  B+      B-sig VSS;
Enddecay

Decay B+sig
1.000   rho+sig   etasig   SVS;
Enddecay
CDecay B-sig

Decay rho+sig
1.000   pi+  pi0sig  VSS;
Enddecay
CDecay rho-sig

Decay etasig
0.5  gamma  gamma  PHSP;
0.5  pi+  pi-  pi0sig  PHSP;
Enddecay

Decay  pi0sig
1.0  gamma  gamma  PHSP;
Enddecay

End
```

Sub-decay	branching fractions
$\mathcal{B}(\rho^+ \to \pi^+\pi^0)$	$\sim 100\%$
$\mathcal{B}(\eta \to \pi\pi\pi^0/\gamma\gamma)$	22.7/39.4%

TABLE III: The sub-decay branching fractions are from the PDG.

3.2. Preselection

We reconstruct the charged B meson in a hierarchical approach starting from the primary particles, namely the charged hadrons $\pi^\pm$ and the photon. Next, we combine two photons to get a π^0 or η, and two charged pion tracks with neutral pion to get a η for the second decay channel of η. A π^+ and a π^0 to reconstruct a ρ^+ candidate. In the end we combine a η and a ρ^+ to reconstruct a charged B meson. The selection requirements are listed in the TABLE IV.

track	$dr < 0.5$cm and $\|dz\| < 2$cm
$\pi^\pm$	$pionID > 0.1$
γ	`tight`
π^0	`eff40_May2020`
η	$0.5 < M_{\gamma\gamma} < 0.57 GeV/c^2$
η	$0.53 < M_{\pi\pi\pi^0} < 0.56 GeV/c^2$
ρ^+	$0.6 < M_{\pi^+\pi^0} < 0.9 GeV/c^2$
B^+	$5.26 < M_{bc} < 5.29 GeV/c^2$
	$\|\Delta E\| < 0.4 GeV$

TABLE IV: signal preselections

3.2.1. Decay mode for $\eta(\to \gamma\gamma)$

After the preselection cuts, some selection for $B^+ \to \rho^+\eta_{\gamma\gamma}$ variables are shown below. The number of fake B^+ candidates is approximately 1.79 times larger than that of true B^+ candidates.

To increase the purity, we planned to veto the fake η and ρ^+ candidates by looking into the γ energy asymmetric and the $\cos\theta_{hel}(\rho^+)$ for each of them.

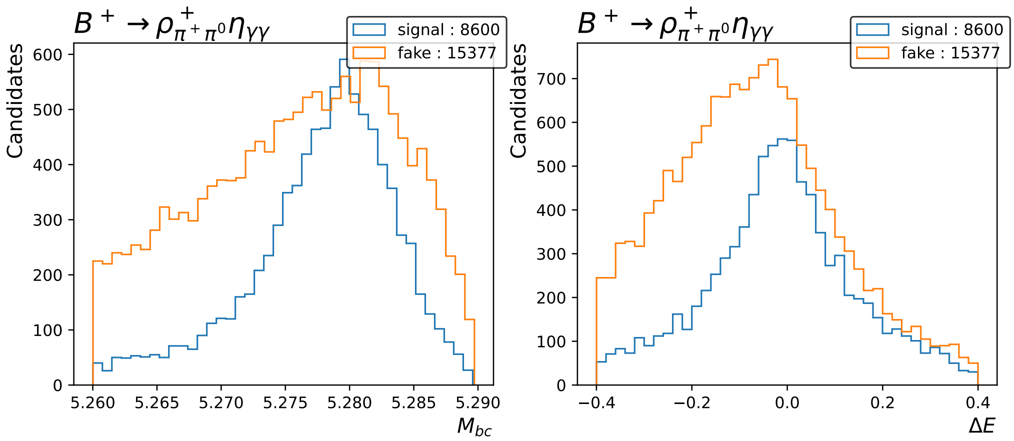

FIG. 1: The distribution of M_{bc} and ΔE of decay channel of $B^+ \to \rho^+\eta_{\gamma\gamma}$

We try to distinguish fake ρ^+ using helicity angle of ρ^+ decay. Helicity angle (θ_{hel}) is defined as the angle between B^+ and π^+ from ρ^+ decay in the ρ^+ rest frame. The cosine of helicity angle (θ_{hel}) is defined below.

$$\cos\theta_{\rm hel}(\rho^+) = \frac{\vec{P}_{\pi^+}\cdot\vec{P}_{B^+}}{|\vec{P}_{\pi^+}||\vec{P}_{B^+}|} \tag{1}$$

The fake ρ^+ candidates account for 60% of all η candidates. An introduced $\cos\theta_{hel}(\rho^+)$ variable can help suppress fake ρ^+ candidates, with $\cos\theta_{hel} > -0.8$ applied as selection cut, nearly 75% fake ρ^+ candidates was rejected, while 84% true ρ^+ candidates remained.

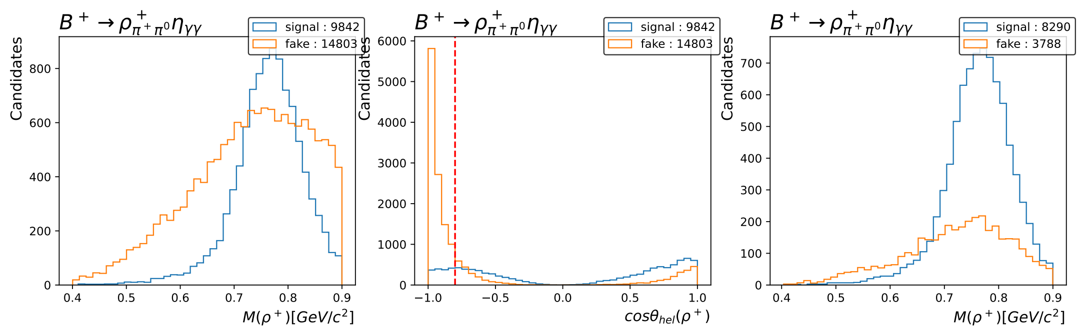

FIG. 2: The mass distribution of ρ^+ of decay channel of $B^+ \to \rho^+\eta_{\gamma\gamma}$ before apply $\cos\theta_{hel} > -0.8$(left), and after(right), with the distribution of $\cos\theta_{hel}$ of ρ^+.

The fake η candidates account for 12% of all η candidates, to reject such fake candidates, introducing energy asymmetry variable($E_{asym} \equiv \frac{|E_{\gamma1}-E_{\gamma2}|}{E_{\gamma1}+E_{\gamma2}}$) can help for suppression. Here, we managed to figure out the ideal selection criteria of E_{asym} by using the figure of merit method, which is defined as $FOM \equiv \frac{S}{\sqrt{S+B}}$, where S is true signal candidates and B is fake one. We found that the maximum figure of merit occurs when applying $E_{asym} < 0.89$, this way, 95% signal η candidates are retained, while nearly 65% fake candidates have been rejected.

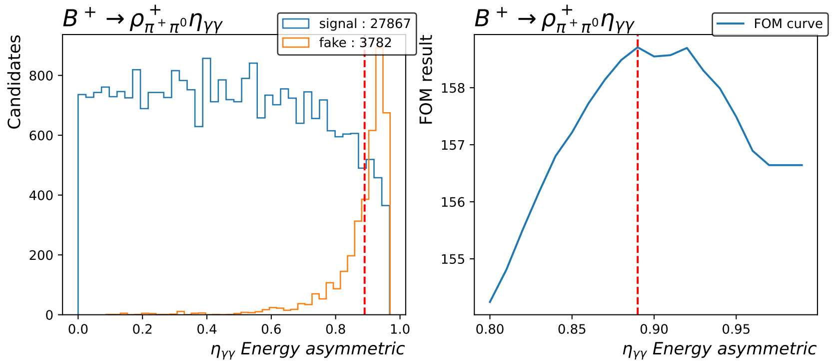

(a)The gamma energy asymmetric distribution in $\eta_{\gamma\gamma}$ channel(left) and the figure of merit curve for finding the ideal selection cut(right).

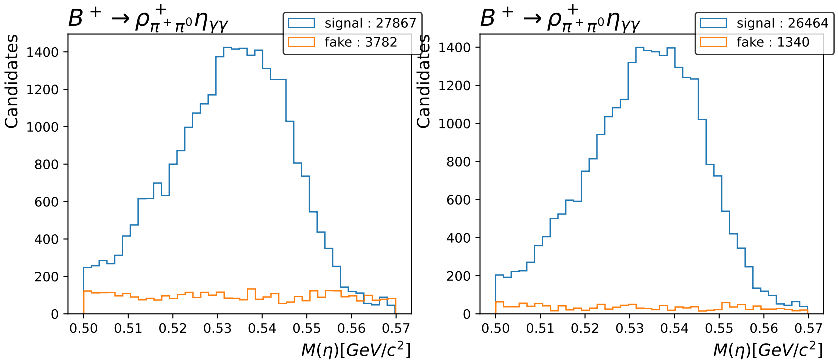

(b)The mass distribution of η before apply cut of energy asymmetric less than 0.89(left), and after(right).

FIG. 3: The figure of merit curve and gamma energy asymmetric distribution(above), and the mass distribution of η (below).

Furthermore, we manage to perform the energy selection criteria to γ_η by figure of merit method with the same definition as we mentioned above. We figure out that the maximum of FOM values occurs when $E(\gamma_\eta) > 0.13\ GeV$ applied.

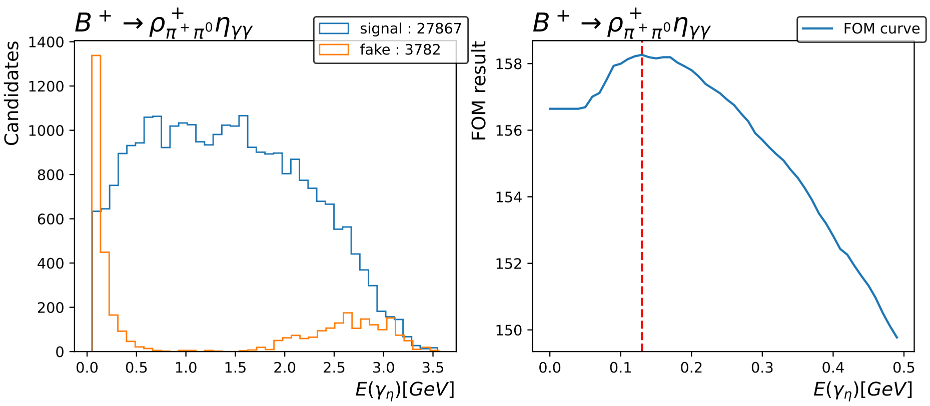

FIG. 4: The energy distribution of γ_η(left) and the FOM curve(right).

3.2.2. Decay mode for $\eta(\to \pi\pi\pi^0)$

After the preselection cuts, some selection for $B^+ \to \eta_{\pi\pi\pi^0}\rho^+$ variables are shown in below. There are many fake B candidates which are approximately 2.1 times larger than true B candidates.

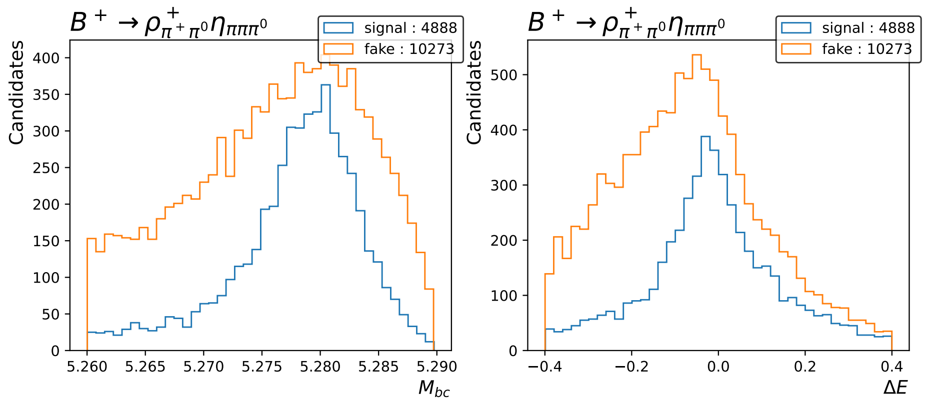

FIG. 5: The M_{bc} ΔE distribution in $\eta_{\pi\pi\pi^0}$ channel.

Again, we try to distinguish fake ρ^+ using helicity angle of ρ^+ decay. The cosine of helicity angle (θ_{hel}) distributions are shown in FIG. 6 and the definition is defined in Eq. 1. An introduced $\cos\theta_{hel}(\rho^+)$ variable can help suppress fake ρ^+ candidates. After we require $\cos\theta_{hel}(\rho^+) > -0.8$, nearly 75% fake ρ^+ candidates has been rejected, while 83% true candidates remained.

The true η candidate accounts for nearly 82% of all the η candidates, set mass windows from 0.53 GeV/c^2 to 0.56 GeV/c^2 for further analysis.

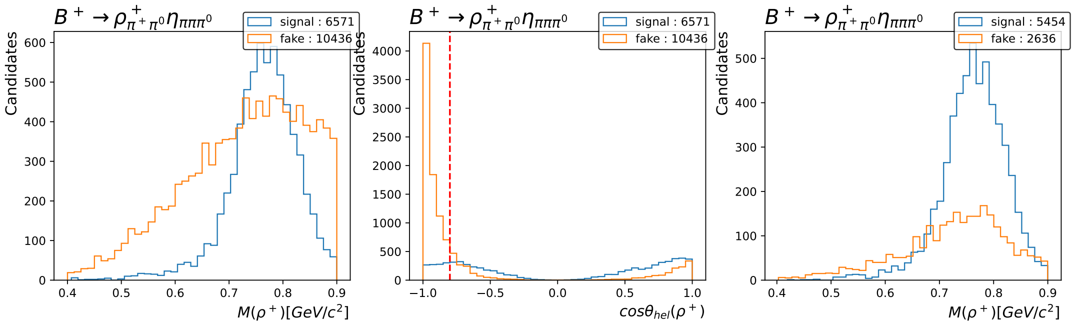

FIG. 6: The mass distribution of ρ^+ before selection(left) and after(right) with the cosine of helicity angle (θ_{hel}) distributions(middle) in $\eta_{\pi\pi\pi^0}$ channel.

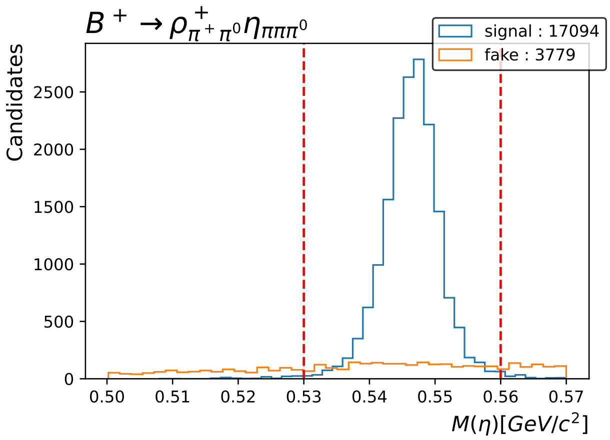

FIG. 7: The mass distribution of $\eta_{\pi\pi\pi^0}$

3.3. Event selection

In order to clean up the selfcross feed, the selections are updated as in the TABLE V. Compablack to the preselection requirements in TABLE IV, the updated parts are marked in black. Till this point, no best candidate selection applied.

track	$dr < 0.5$cm and $\|dz\| < 2$cm
$\pi^{\pm}$	$pionID > 0.1$
γ	`tight`
π^0	`eff40_May2020`
η	$0.5 < M_{\gamma\gamma} < 0.57GeV/c^2$
η	$0.53 < M_{\pi\pi\pi^0} < 0.56GeV/c^2$
ρ^+	$0.6 < M_{\pi^+\pi^0} < 0.9GeV/c^2$
	$cos\theta_{hel} > -0.8$
$\eta_{\gamma\gamma}$	energy asymmetry < 0.9
B^+	$5.26 < M_{bc} < 5.29GeV/c^2$
	$\|\Delta E\| < 0.4GeV$

TABLE V: Signal selections after cleaning up of self-cross feed.

3.4. Best candidate selection

In order to choose the best B candidates in one collision event, we introduce a variable `chiProb` from treefit. Before best candidate selection the average multiplicity per event for mode $B^+ \to \eta_{\gamma\gamma}$ is 1.35 and for mode $B^+ \to \eta_{\pi\pi\pi^0}$ is 1.50. Around 86.67% of correctly reconstructed signal for mode $B^+ \to \eta_{\gamma\gamma}$ and 84.00% for mode $B^+ \to \eta_{\pi\pi\pi^0}$ selected by the highest `chiProb` requirement. The comparison of the purity and the signal efficiency after skim selection/Clean-up for self-cross feed/Highest `chiProb` requirement are shown in the TABLE VI. The purity is $N_{sig}/N_{candidates}$ and signal efficiency is $\epsilon_{sig} = N_{sig}/N_{gen}$.

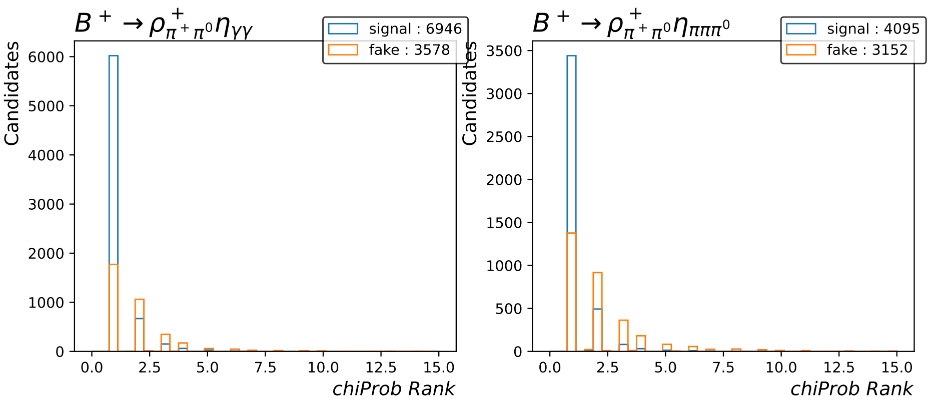

FIG. 8: The chiProb distribution of these 2 channels.

	$B^+ \to \rho^+\eta_{\pi\pi\pi^0}$		$B^+ \to \rho^+\eta_{\gamma\gamma}$		Total	
	Purity	ϵ_{sig}	Purity	ϵ_{sig}	Purity	ϵ_{sig}
Skim selection	32.24%	9.78%	35.87%	17.20%	34.46%	13.49%
Clean-up for sxf	56.51%	8.19%	66.08%	13.89%	62.17%	11.04%
Highest `chiProb`	71.41%	6.88%	77.26%	12.04%	75.03%	9.46%

TABLE VI: The comparison of the purity and the signal efficiency after skim selection/Clean-up for selfcross feed/Highest.

After best candidate selection, the signal distribution of M_{bc} and ΔE are shown in the FIG. 9 . The effeciency, purity and the number of expected events are shown in the TABLE. **??**.

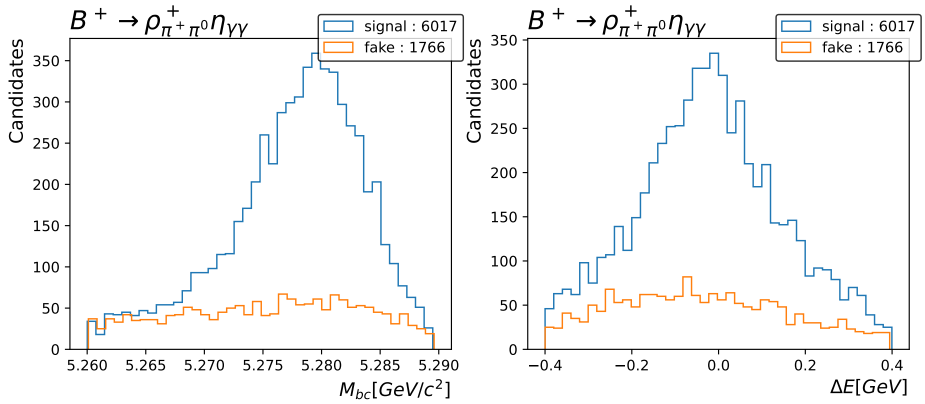

(a)The M_{bc} ΔE distribution of $\eta_{\gamma\gamma}$ channel.

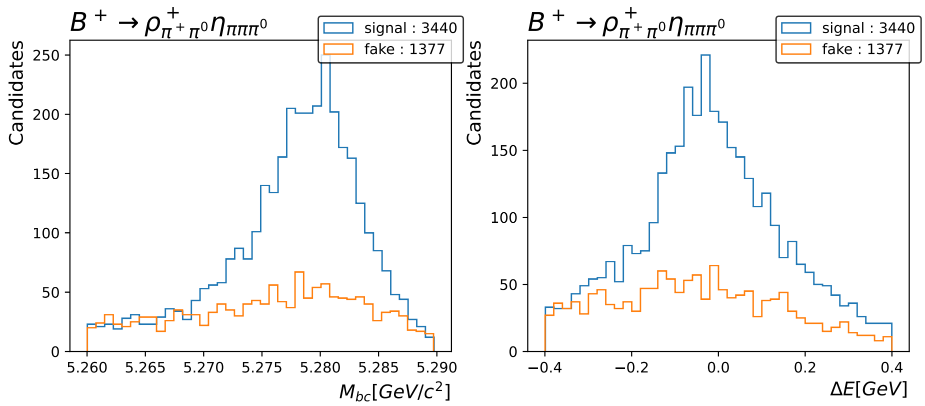

(b)The M_{bc} ΔE distribution of $\eta_{\pi\pi\pi^0}$ channel.

FIG. 9: The M_{bc} ΔE distribution of 2 channels after BCS selection.

4. EVENT SELECTION-BELLE

4.1. Reconstruction

The signal MC events for Belle use the decay tables shown below. We generated 460000 events, of which 50% are for $B^+ \to \rho^+\eta(\to \gamma\gamma)$ and the other 50% are for $B^+ \to \rho^+\eta(\to \pi\pi\pi^0)$. The sub-branching fractions which come from PDGLive[8] are listed in the TABLE VII. These values will be used later when calculating the expected number of events.

```
Alias      etasig     eta

Alias       rho+sig    rho+
Alias       rho-sig    rho-

Alias       B+sig     B+
Alias       B-sig     B-


#

Decay Upsilon(4S)
0.5  B+sig   B-   VSS;  #208
0.5  B+      B-sig VSS;  #208
Enddecay

Decay B+sig
1.000   rho+sig   etasig   PHOTOS SVS;   #4767
Enddecay

Decay B-sig
1.000   rho-sig   etasig   PHOTOS SVS;  #4767
Enddecay

Decay rho+sig
1.000   pi+  pi0  VSS;  #5494
Enddecay

Decay rho-sig
1.000   pi-  pi0  VSS;  #5494
Enddecay

Decay etasig
0.5  gamma  gamma  PHSP;    #5461
0.5  pi+  pi-  pi0  PHOTOS ETA_DALITZ;  #5464
Enddecay

End
```

Sub-decay	branching fractions
$\mathcal{B}(\rho^+ \to \pi^+\pi^0)$	$\sim 100\%$
$\mathcal{B}(\eta \to \pi\pi\pi^0/\gamma\gamma)$	22.7/39.4%

TABLE VII: The sub-decay branching fractions are from the PDG.

4.2. Signal Selection Strategy

4.2.1. preselection

We reconstruct the charged B meson in a hierarchical approach starting from the primary particles, namely the charged hadrons $\pi^{\pm}$ and the photon. Next, we combine two photons to get a π^0 or η, and two charged pion tracks with neutral pion to get a η for the second decay channel of η. A π^+ and π^0 to reconstruct a ρ^+ candidate. In the end we combine a η and a ρ^+ to reconstruct a charged B meson. The selection requirements are listed in the TABLE VIII.

track	$dr < 0.5$cm and $\|dz\| < 2$cm
$\pi^{\pm}$	$kIDBelle < 0.4$
γ	$E_{\gamma} > 0.05$ GeV
π^0	$0.11 < M_{\pi^0} < 0.16$ GeV
η	$0.5 < M_{\gamma\gamma} < 0.57$ GeV/c^2
η	$0.53 < M_{\pi\pi\pi^0} < 0.56$ GeV/c^2
ρ^+	$0.6 < M_{\pi^+\pi^0} < 0.9$ GeV/c^2
	$cos\theta_{Heli} > -0.8$
$\eta_{\gamma\gamma}$	energy asymmetry < 0.9
B^+	$5.26 < M_{bc} < 5.29$ GeV/c^2
	$\|\Delta E\| < 0.4$ GeV
	ChiProbRank = 1 in tree fit (Best candidates selection)

TABLE VIII: signal preselections

4.2.2. $\eta_{\gamma\gamma}$ Energy asymmetric and ρ^+ cosine helicity angle

An introduced energy asymmetry variable can help suppress fake η candidates. After we require $E_{asym} < 0.9$, The fake η candidates account for 17% of all η candidates, to reject fake candidates, introducing energy asymmetry variable can help for suppression. Here, we managed to figure out the selection criteria of E_{asym} by using the figure of merit (FOM) method, which is defined as $FOM = \frac{\sqrt{S}}{\sqrt{S+B}}$, where S is number of true signal candidates and B is fake reconstructed ones (self-cross-feed, scf). We selected the maximum figure of merit point and applying $E_{asym} < 0.9$. Then, 97% true η candidates are retained, while nearly 75% fake candidates have been rejected.

$$E_{asym} \equiv \frac{|E_{\gamma_1} - E_{\gamma_2}|}{(E_{\gamma_1} + E_{\gamma_2})} \tag{2}$$

We try to distinguish fake ρ^+ using helicity angle of ρ^+ decay. An introduced $\cos\theta_{hel}(\rho^+)$ variable can help suppress fake ρ^+ candidates. Helicity angle (θ_{hel}) is defined as the angle between B^+ and π^+ from ρ^+ decay in the ρ^+ rest frame. With selection criteria applied, 83% true ρ^+ candidates are retained, while nearly 68% fake ρ^+ candidates have been rejected.

The cosine of helicity angle (θ_{hel}) is defined as.

$$\cos\theta_{\text{hel}}(\rho^+) \equiv \frac{\vec{P}_{\pi^+}\cdot\vec{P}_{B^+}}{|\vec{P}_{\pi^+}||\vec{P}_{B^+}|} \tag{3}$$

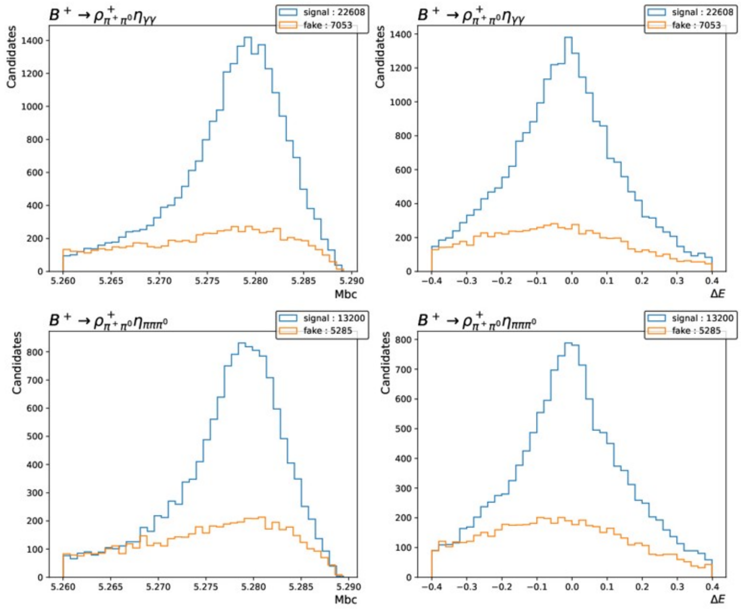

FIG. 10: The M_{bc} and ΔE distribution of $B^+ \to \rho^+\eta$

.

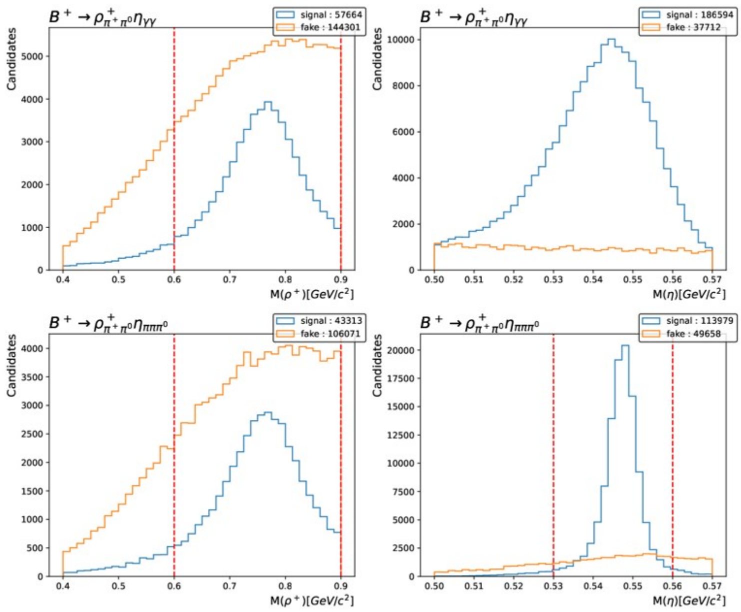

FIG. 11: The mass distribution of ρ^+ and η

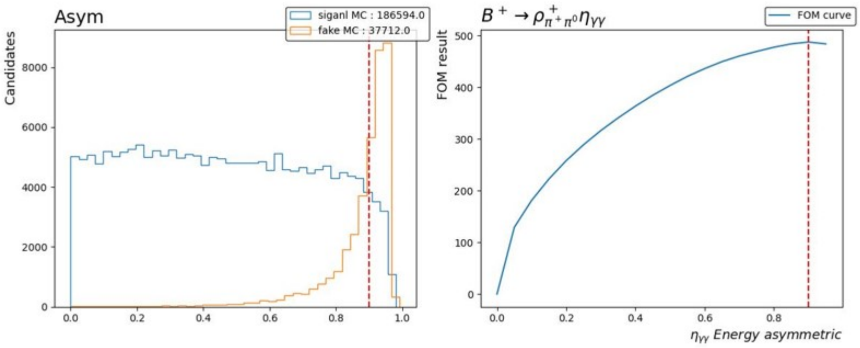

FIG. 12: The energy asymmetric of $\eta_{\gamma\gamma}$

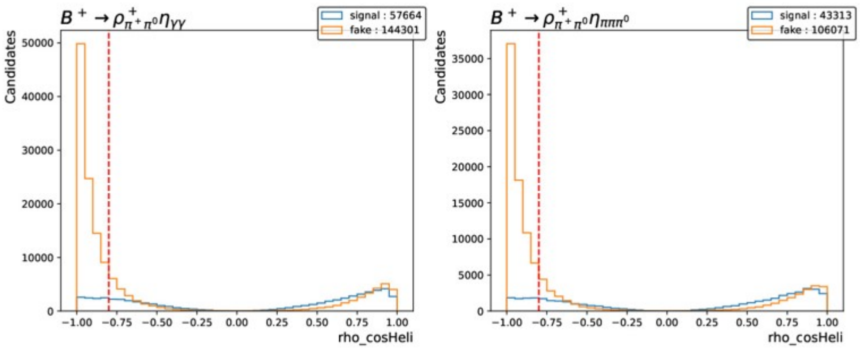

FIG. 13: The cosine helicity angle of ρ^+

4.2.3. Best candidate selection

In order to choose the best B candidates in one collision event, we introduce a variable `chiProb` from treefit. Before best candidate selection the average multiplicity per event for mode $B^+ \to \rho^+\eta_{\gamma\gamma}$ is 1.597, and $B^+ \to \rho^+\eta_{\pi\pi\pi^0}$ is 1.715. Around 62.5% of correctly reconstructed signal for mode $B^+ \to \rho^+\eta_{\gamma\gamma}$ and 55.5% for mode $B^+ \to \rho^+\eta_{\pi\pi\pi^0}$ selected by the highest `chiProb` requirement. The purity is $\frac{N_{signal}}{N_{candidates}}$ and signal efficiency is $\epsilon_{sig} = \frac{N_{signal}}{N_{generate}}$.

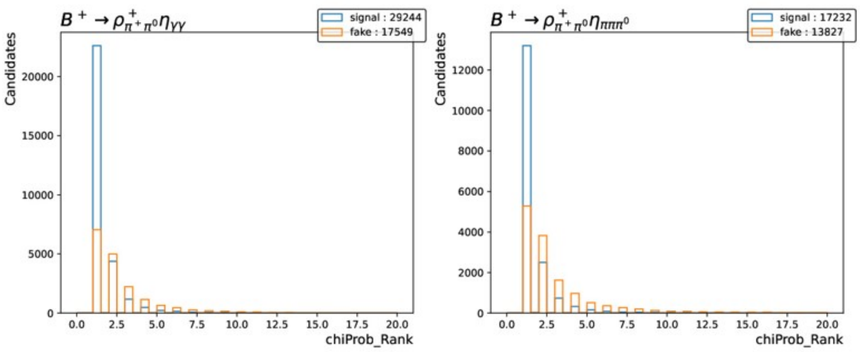

FIG. 14: The best candidates rank for 2 channels

4.2.4. *Sum up of Signal MC*

We generated 460K events for signal MC study, getting 35808 signal B candidates and 12338 self-cross-feed passing the selection criteria, the filter efficiency and the cut flow table shown as below.

Filter	# sig remain	# scf remain	sig remain (%)	scf remain (%)
ρ^+ mass	68729	215791	91.81	81.39
η mass	73612	243129	98.34	91.7
M_{bc} ΔE	62495	164385	83.49	62.0
Asym < 0.9	72630	240045	97.03	90.53
$\rho^+ \cos$ HelicityAngle	62349	95579	83.29	36.05
best rank	51981	62587	69.44	23.6

TABLE IX: Selection efficiency for different filters, the number of original signal entries is 74856 and the one of self-cross-feed is 265146

Filter	**# of signal entries**	**# of self-cross-feed entries**
original	74856.0	265146.0
ρ^+ mass	68729.0	215791.0
η mass	67600.0	197281.0
M_{bc} ΔE	59279.0	130459.0
Asym < 0.9	57502.0	118522.0
$\rho^+ \cos$ HelicityAngle	46476.0	31376.0
best rank	35808.0	12338.0
remained (%)	47.84	4.65

TABLE X: Cut Flow Table

String	generated	selected	signal	purity	ε	Expected
$B^+ \to \rho_{\pi^+\pi^0}\eta_{\pi\pi\pi^0}$	230000.0	18485	13200	0.7141	0.0574	99.63
$B^+ \to \rho_{\pi^+\pi^0}\eta_{\gamma\gamma}$	230000.0	29661	22608	0.7622	0.0983	295.62
Total	460000.0	48146	35808	0.7437	0.0778	369.01

TABLE XI: The sum up table of signal MC

4.3. Background Study

4.3.1. generic MC veto

We generated 1 stream neutral, charged B, and continuum background for further study, then we found out that the continuum part contribute the most of the background. First, try π^0 veto to reject fake candidates η on the generic side. The π^0 veto rejection region is [0.125, 0.145].

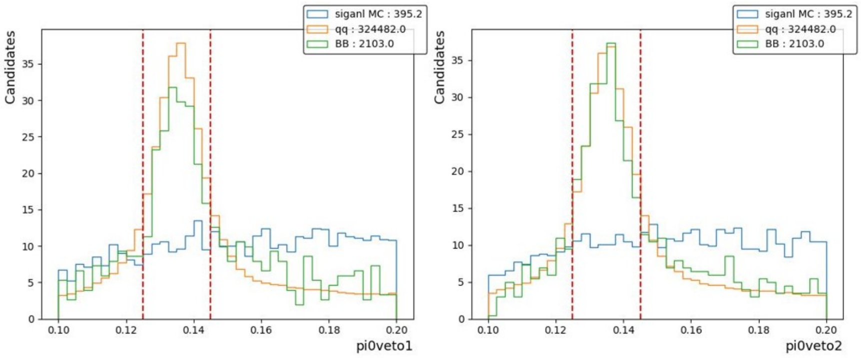

FIG. 15: The π^0 veto for generic background

4.3.2. Continuum Suppression

We employed XGBoost as our Multivariate Analysis (MVA) model. By analyzing the variable importance diagram, we identified cosTBTO as the most significant feature, the AUC score was 0.976 for the training sample and 0.957 for the testing sample. These results were achieved with a learning rate of 0.1, a maximum depth of 5, 200 estimators, and gamma set to 0. The hyperparameters were determined using GridSearchCV.

Furthermore, We get 204.3 signal candidates, 4705.0 continuum candidates and 269.0 generic B candidates that pass the π^0 veto and the C_{cs} selection as MVA, for the self-generated signal that has been rescaled to the amount of real data.

The C_{cs} suppression region decided by using the figure of merit method ($FOM = \frac{S}{\sqrt{S+B}}$).

Filter	# signal entries	# mixed entries	# charged entries	# charm entries	# uds entries
original	35808.0	952.0	1151.0	59219.0	265263.0
pi0veto	20200.0	447.0	437.0	22179.0	101389.0
MVA (> 0.8)	15625.0	139.0	130.0	1157.0	3548.0
remained (%)	43.64	14.6	11.29	1.95	1.34

TABLE XII: Cut flow table of each background source

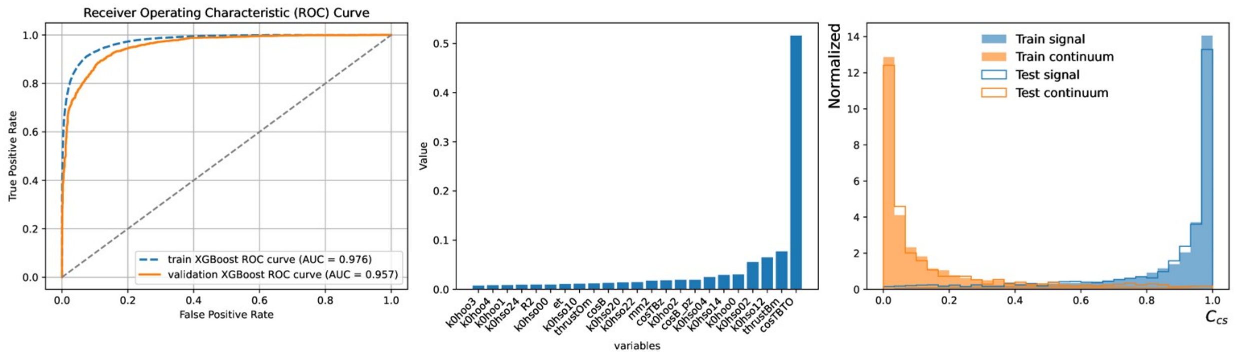

FIG. 16: The ROC curve (left), the variables importance(middle), and the C_{cs} of the training model(right).

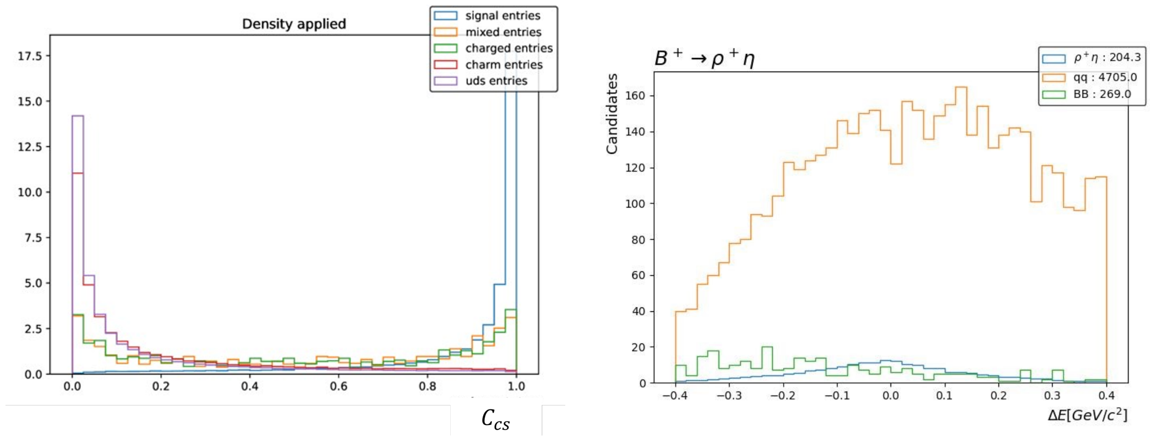

FIG. 17: The distribution of C_{cs} of each background source passing the training model in the background sample (left), and the ΔE distribution of signal, generic, and continuum background sample (right).

5. SUMMARY

For the MC samples in Belle and Belle II, the event selections, clean-up for selfcross feed and best candidate selection are decided. The number of expected events of decay mode $B^+ \to \rho^+\eta$ in Belle II and Belle has been obtained, . Based on the above results, there is a chance to obtain an observation of this decay mode in Belle II; this indicates that continuing the measurements of branching fractions and CP asymmetry of $B^+ \to \eta\rho^+$ decays is worthwhile.

We were currently planning using MC_16 run dependent sample in Belle II once more to look into the difference of Belle II and Belle data set.

References

1. Beneke, M. & Neubert, M. Flavor-singlet B-decay amplitudes in QCD factorization. *Nuclear Physics B* **651,** 225–248. `https://www.sciencedirect.com/science/article/pii/S055032130201091X` (2003).
2. Akeroyd, A. G., Chen, C.-H. & Geng, C.-Q. $B \to \eta^{(\prime)}(l^- \overline{\nu}_l, l^+l^-, K, K^*)$ decays in the quark-flavor mixing scheme. *Phys. Rev. D* **75,** 054003. `https://link.aps.org/doi/10.1103/PhysRevD.75.054003` (5 2007).
3. Beneke, M. & Neubert, M. QCD factorization for B→PP and B→PV decays. *Nuclear Physics B* **675,** 333–415. `https://www.sciencedirect.com/science/article/pii/S0550321303007752` (2003).
4. Wang, W., Wang, Y.-M., Yang, D.-S. & Lü, C.-D. Charmless two-body $B_{(s)} \to VP$ decays in soft collinear effective theory. *Phys. Rev. D* **78,** 034011. `https://link.aps.org/doi/10.1103/PhysRevD.78.034011` (3 2008).
5. Chiang, C.-W. & Zhou, Y.-F. Flavor symmetry analysis of charmless B → VP decays. *Journal of High Energy Physics* **2009,** 055. `https://dx.doi.org/10.1088/1126-6708/2009/03/055` (2009).
6. Schümann, J. *et al.* Search for B decays into $\eta^{'}p$, $\eta^{'}K^*$, $\eta^{'}\phi$, $\eta^{'}\omega$ and $\eta^{'}\eta^{(\prime)}$. *Phys. Rev. D* **75,** 092002. `https://link.aps.org/doi/10.1103/PhysRevD.75.092002` (9 2007).
7. Del Amo Sanchez, P. *et al.* B-meson decays to $\eta^{'}\rho$, $\eta^{'}f_0$, and $\eta^{'}K^*$. *Phys. Rev. D* **82,** 011502. `https://link.aps.org/doi/10.1103/PhysRevD.82.011502` (1 2010).
8. Navas, S. *et al.* Review of Particle Physics. *Phys. Rev. D* **110,** 030001. `https://link.aps.org/doi/10.1103/PhysRevD.110.030001` (3 2024).